Type of manuscript: Article

Supporting Information

Fabrication of TiO_2 trapped meso/macroporous g-C_3N_4 heterojunction photocatalyst and understanding for its enhanced photocatalytic activity based on the optical simulation analysis

Wanbao Wu, [a,1] Xu Li, [a,1] Zhaohui Ruan, [b,1] Yudong Li, [a] Xianzhu Xu, [a] Yuan Yuan,[*b] Kaifeng Lin[*a]

[a]MIIT Key Laboratory of Critical Materials Technology for New Energy Conversion and Storage, School of Chemistry and Chemical Engineering, Harbin Institute of Technology, Harbin 150001, China. Emails of corresponding authors: linkaifeng@hit.edu.cn

[b]School of Energy Science and Engineering, Harbin Institute of Technology, Harbin 150001, China. Emails of corresponding authors: yuanyuan83@hit.edu.cn

Experimental Section

Characterization

X-ray Diffraction (XRD) measurement was conducted to characterize crystal structure of as-prepared samples on Bruker D8 Advance diffractometer by using Cu Ka radiation. Fourier Transform Infrared (FT-IR) spectra was tested in Perkin Elmer 100 spectrometer. The thermal stability of samples was performed by using thermogravimetric (TG) analysis with NETZSCH Instrument STA 449 F3 Jupiter. X-ray photoelectron spectra (XPS) were was used to characterize the chemical state of elements in the as-prepared samples with PHI 5700 ESCA system equipped with an A1 Kα radiation as a source ($h\upsilon$ = 1486.6 eV). A Hitachi S-4800 model microscope was adoped to observe the morphologies of as-prepared samples. Transmission electron microscopy (TEM) images were obtained on a Topcon 002B. UV–vis diffuse reflection spectra ($BaSO_4$ as the reflectance standard) was analyzed on Perkin Elmer Lambda 750 spectrophotometer from 200 to 800 nm. The BET surface area and pore-size distribution were recorded on Micromeritics ASAP2020. Meanwhile, the photoluminescence (PL) measurement were performed using PerkinElmer LS-55 with 375 nm as excitation wavelength under liquid nitrogen conditions.

Supporting Figures (S1-S12), Tables S1.

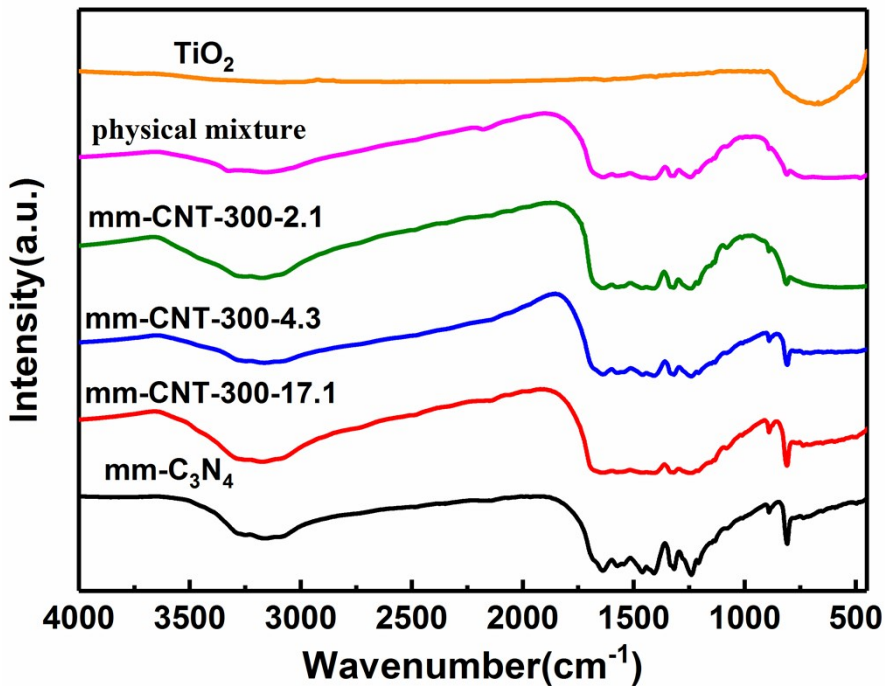

Fig. S1 Fourier transform infrared (FI-IR) spectra of TiO_2, physical mixture, mm-C_3N_4, and mm-CNT heterojunctions respectively

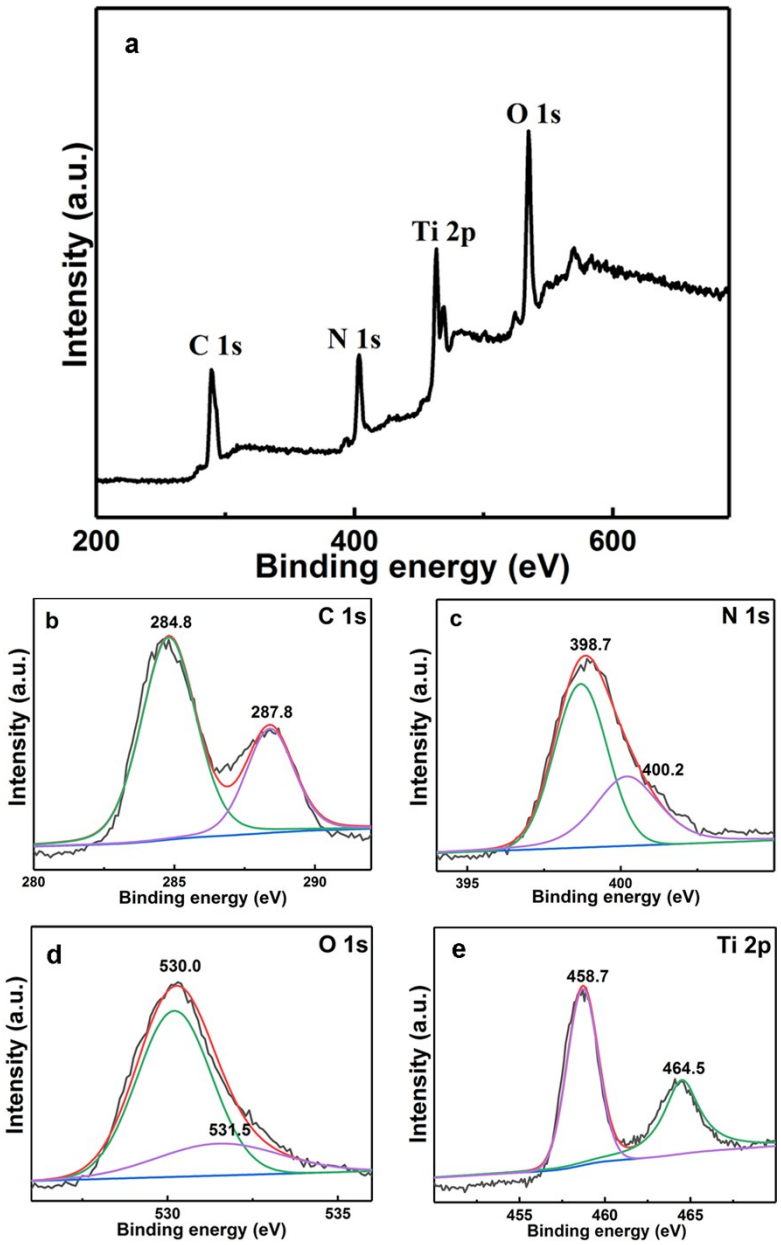

Fig. S2 (a) XPS survey spectrum of mm-CNT-300-4.3 and high-resolution spectra of (b) C1s, (c) N1s, (d) O1s and (e) Ti2p for mm-CNT-300-4.3.

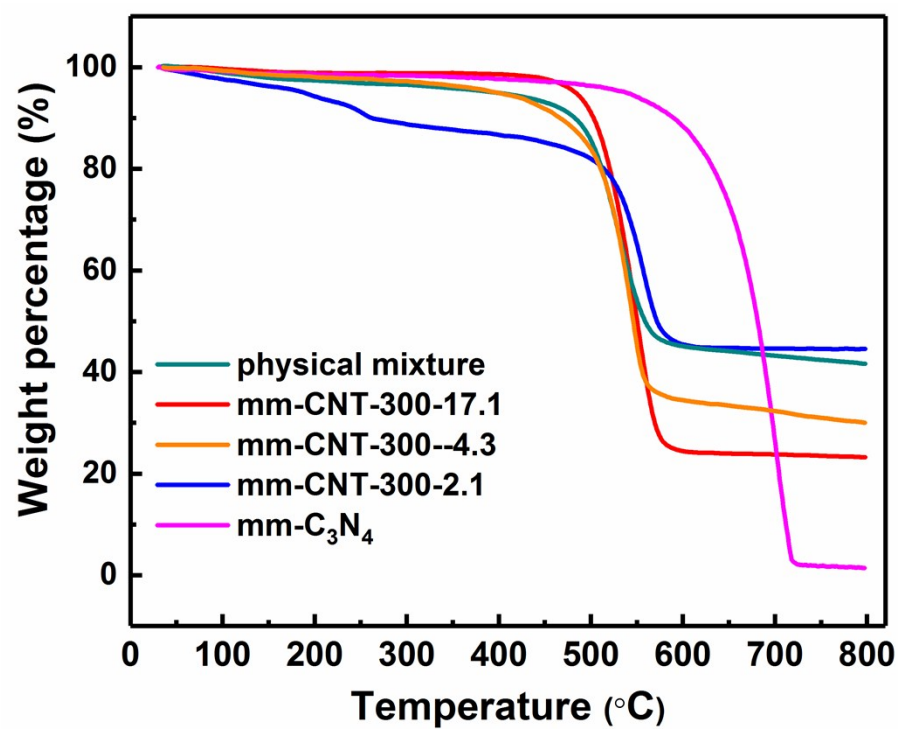

Fig. S3 TGA curves for the physical mixture, mm-C_3N_4 and mm-CNT heterojunctions respectively.

Table S1 physical properties of the as-prepared samples.

Sample	mm-C_3N_4	mm-CNT-300-2.1	mm-CNT-300-4.3	mm-CNT-300-17.1	physical mixture
S_{BET} (m^2g^{-1})	37.5	55.0	63.6	71.7	22.5
Pore Volume (cm^3g^{-1})	0.28	0.28	0.29	0.30	0.14
Average pore size (nm)	36	24	20	27	32

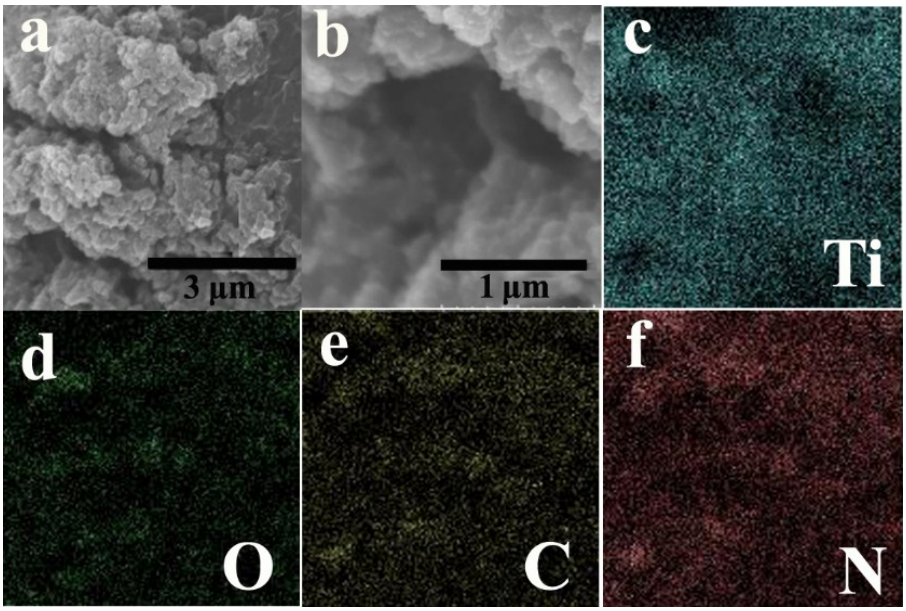

Fig. S4 (a-b) SEM images and (c-f) EDS mapping of mm-CNT-300-4.3.

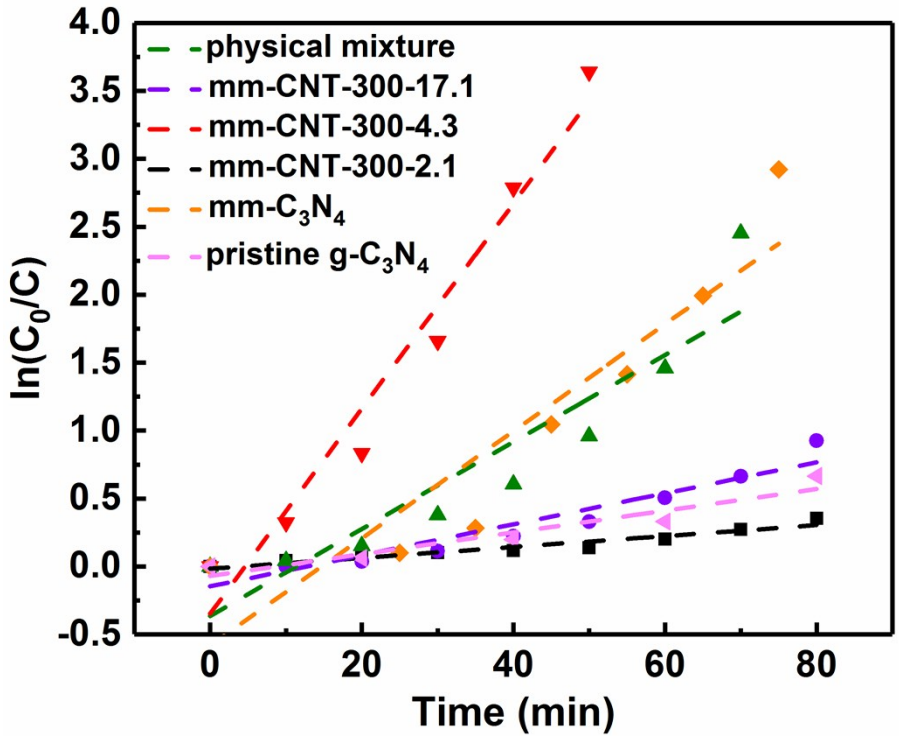

Fig. S5 Kinetic curves for the RhB photodegradation over mm-C_3N_4, physical mixture and mm-CNT heterojunctions respectively.

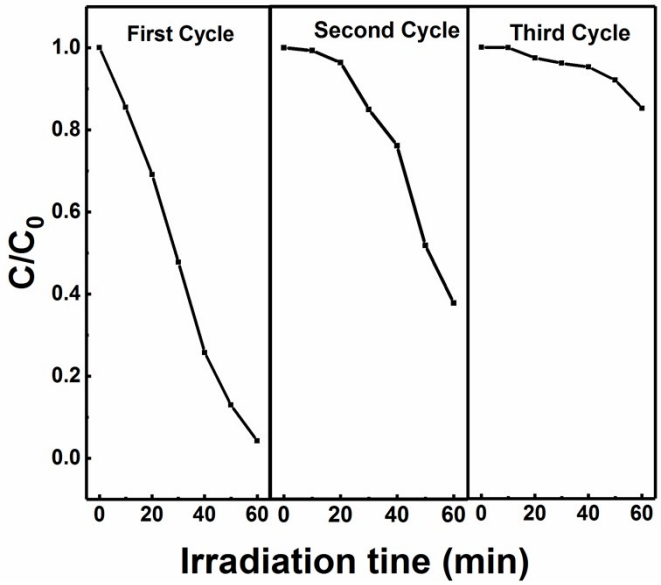

Fig. S6 Cycle runs of physical mixture for degradation of RhB under visible-light irradiation.

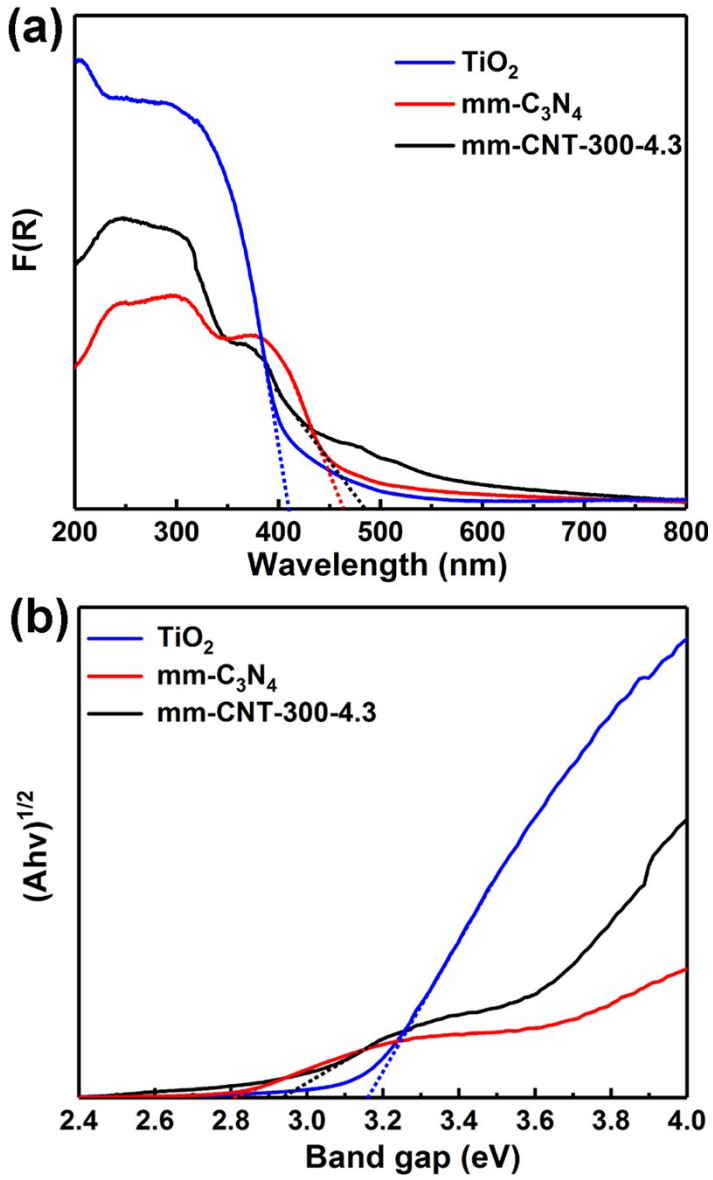

Fig. S7 (a) UV−vis absorption spectra and (b) the corresponding Kubelka−Munk transformed reflectance spectra of mm-C_3N_4, TiO_2 and mm-CNT-300-4.3.

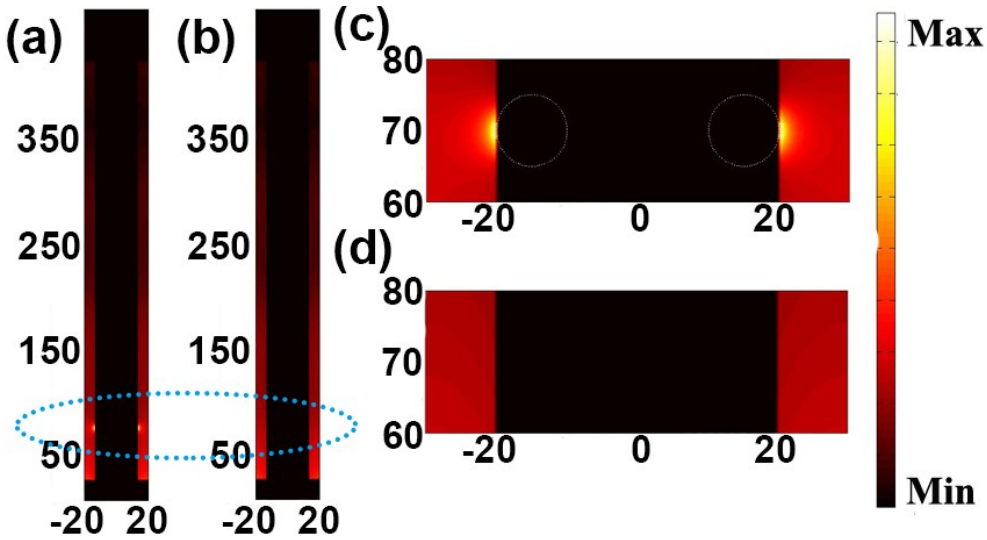

Fig. S8 The generation rate of photo-induced carriers in x-z plane (a) TiO_2 particles are placed inside the pores of mm-C_3N_4, (b) pure mm-C_3N_4, (c) and (d) are partial enlargement of (a) and (b), respectively.

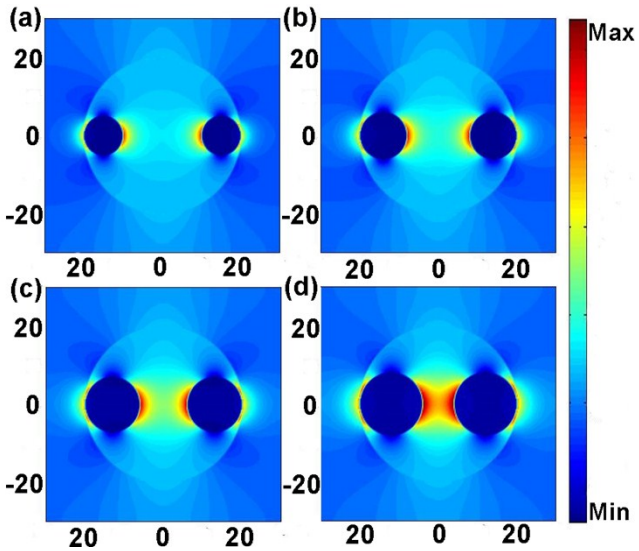

Fig. S9 Electric field intensity distribution in x-y plane when the diameter of the TiO_2 particles are (a) d=10 nm, (b) d=12 nm, (c) d=14 nm, (d) d=16 nm.

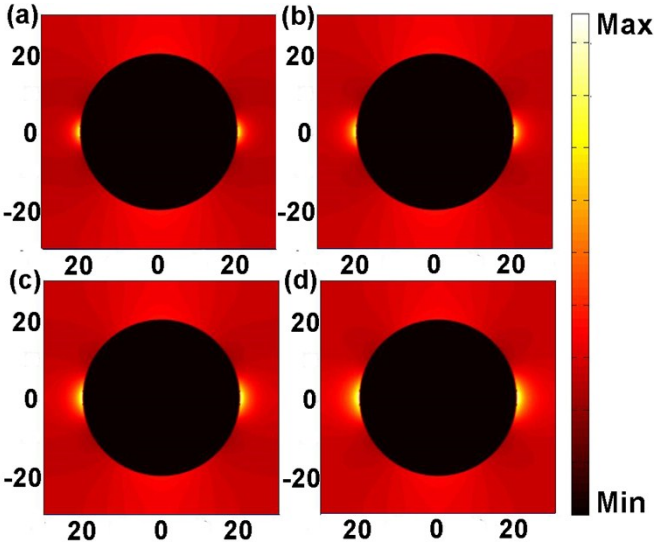

Fig. S10 Optical absorption intensity distribution in x-y plane when the diameter of the TiO_2 particles are (a) d=10 nm, (b) d=12 nm, (c) d=14 nm, (d) d=16 nm.

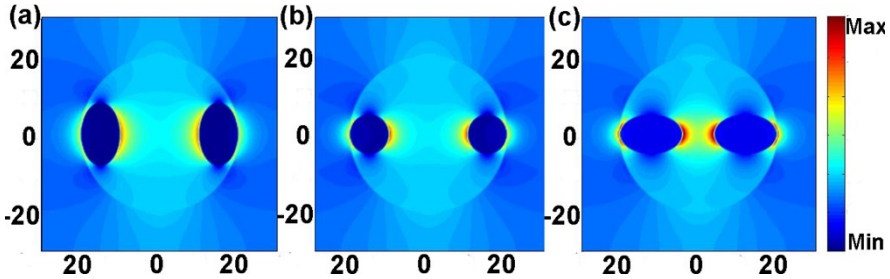

Fig. S11 Electric field intensity distribution in x-y plane (a) TiO_2 particles are stretched in the y direction, (b) TiO_2 particles are kept to be a regular sphere, (c) TiO_2 particles are stretched in the x direction.

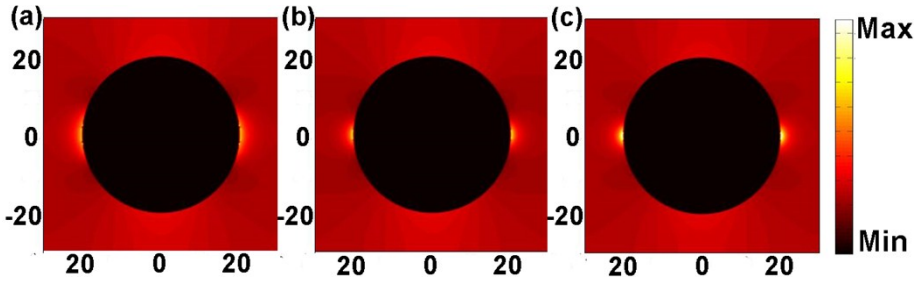

Fig. S12 Electric field intensity distribution in x-y plane (a) TiO_2 particles are stretched in the y direction, (b) TiO_2 particles are kept to be a regular sphere, (c) TiO_2 particles are stretched in the x direction.